International Journal of Thermophysics (2023) 44:1
https://doi.org/10.1007/s10765-022-03112-y

Heat Transfer and Flow Analysis in a Circular Tube Equipped with Triangular Helical Strip Inserts Under Turbulent Flow Conditions for the Application of Boiler

Tushar Adgale[1] · Prabhakar Zainith[1] · Niraj Kumar Mishra[1] · Anshul Sharma[2]

Received: 18 June 2022 / Accepted: 3 October 2022 / Published online: 21 October 2022

Abstract

In the present study, an experimental investigation was carried out for the Nusselt number, friction factor and thermal performance factor using triangular helical strip inserts. For the experimentation air was considered as flowing fluid medium with Reynolds number ranging from 37 500 to 52 000. For present study helical strip inserts of widths 5 mm, 7.5 mm, and 10 mm were considered and varied with two pitches i.e., single pitch (i.e., w = P) and double pitch (i.e., w = 2P) i.e., 5 mm width strip with 5 mm and 10 mm pitch, 7.5 mm width strip with 7.5 mm and 15 mm pitch, 10 mm width strip with 10 mm and 20 mm pitch. In addition, the experimentation was carried out considering two passes of test section to analyze the thermo-hydraulic characteristics. Experimental results exhibited that heat transfer and thermal performance of the helical inserted tube were expressively improved compared to plain tube. The Nusselt number of helical strip inserts is more for inserts with lower width, tighter pitch for all geometries. Nusselt number ratio was 1.45–2.05 times for single pass and 1.55–2.45 times that of plain tube. The friction factor is lower for inserts with higher pitch. The friction factor is high insert with higher width. The friction factor enhancement ratio is high for strips with more significant number of passes, tighter pitch and more width. The thermo-hydraulic performance of the helical strip insert improves for high number of passes, lower width, lower pitch. Moreover, the thermal enhancement factor (TEF) was in the range of 1.01–2.03 and 1.08–2.41 for single pass and double pass, respectively.

Keywords Friction factor · Heat transfer enhancement · Helical strip insert · Nusselt number · Thermal enhancement factor

✉ Niraj Kumar Mishra
nkm@nituk.ac.in; nkm.iitg@gmail.com

[1] Department of Mechanical Engineering, National Institute of Technology Uttarakhand, Garhwal, Srinagar 246174, India

[2] Department of Mechanical Engineering, Thapar Institute of Engineering & Technology, Patiala, Punjab 147004, India

Abbreviations

f	Friction factor
fa	Friction factor of turbulator
fo	Friction factor of plain tube
$f_{a(thsi)}$	Friction factor for triangular helical strip inserts
Nu	Nusselt number
Nu_a	Nusselt number of turbulator
Nu_0	Nusselt number of plain tubes
$Nu_{a(thsi)}$	Nusselt number for triangular helical strip inserts
OER	Overall enhancement ratio
P	Pitch (mm)
1P	Single Pitch of helical strip insert
2P	Double Pitch of helical strip insert
t	Thickness (mm)
w	Width of helical strip insert (mm)
η	Thermal enhancement factor (TEF)
Re	Reynolds number
Q	Heat transfer (W)
k	Thermal conductivity ($W \cdot m^{-1} \cdot K^{-1}$)
u	Velocity ($m \cdot s^{-1}$)
T	Temperature (K)
D	Diameter of pipe (m)
V	Voltage (v)
I	Current (A)
ΔP	Pressure difference ($N \cdot m^{-2}$)
h	Heat transfer coefficient ($W \cdot m^{-2} \cdot K^{-1}$)
$\dot{m}$	Mass flow rate ($kg \cdot s^{-1}$)
μ	Dynamic viscosity (Pa·s)
ρ	Density ($kg \cdot m^{-3}$)
C_p	Specific heat of air ($J \cdot kg^{-1} \cdot K^{-1}$)
L	Length of tube (m)
A_s	Surface area of tube (m^2)
W_R	Width ratio
P_R	Pitch ratio

1 Introduction

Typically, the heat enhancement methods involving turbulators lead to increase of friction losses which directly results in increase of pumping power and thus operation cost of the equipment. Hence, while selecting a specific configuration of turbulator, there should be trade-off between heat transfer enrichment and pressure drop to optimize overall cost of heat exchanger. Generally, the geometrical and dimensional configurations govern the thermo-hydraulic performance of turbulators. The presented study comprises important and recent experimental investigation

studies performed by numerous investigators which would be useful for heat transfer enhancement techniques.

Generally, the heat exchanging devices underperform due to formation of thermal boundary layer of the fluids circulating in the system which affects the heat transfer coefficient and ineffective utilization of heating surface area. Formation of swirl flow and secondary flow in system, destructs thermal boundary layer formation, increases flow residence time, increases heat transfer coefficient, and gives effective output with low or optimum heat transfer area which also leads to cost savings [1–6]. Thus, the heat transfer enhancement by creating swirl flow can be done by either active or passive methods. Active methods involve use of peripheral power viz. fluid injection, vibration etc.

In passive methods the flow disruption is done without use of any external energy either by use of protracted, irregular surfaces or insertion of turbulators. Mostly passive heat transfer augmentation techniques are preferred due to low economics in manufacturing, maintenance and operating costs. The high intensity turbulent swirl flow creates vortex formation, disrupting formation of boundary layer, surge in residence period of fluid flow, churning and better mixing of fluid, high rate of temperature and heat transfer and increase of heating surface area leads to promote high convection heat transfer rate. The increase in friction factor is due to augmented surface area causing reduction in flow area or blockage in path of flow, dissipation of the dynamic pressure due to flow turbulence, secondary flow, and increase in longer flow path leading to increased residence time.

Eiamsa-ard et al. [7] performed experiments for short-length twisted tape. These tapes generated weak swirl intensity at downstream flow due to which, thermal–hydraulic performance of short length tapes was observed to be inferior to full-length twisted tape. Eiamsa-ard et al. [8] experimented and considered the effect of typical twisted tape insert having full length and regularly spaced inserts (RS-TT) observing that decrease in twist ratio and space ratio increased friction factor and heat transfer. For same space ratio, tapes with tighter twist ratio performed better. Also, noted that RS-TTs generated intermittent swirl intensity at downstream flow due to which augmentation of RS-TTs was observed to be inferior to full-length tape. Ahamed et al. [9] investigated the heat transfer coefficient for perforate twisted experimentally. Bhuiya et al. [10] experimentally observed better performance for tape with perforation ratio of 4.5. Bhuiya et al. [11] scrutinized a study experimentally for perforated double counter twisted tape, noting better performance for tape with perforation ratio of 4.6. Bhuiya et al. [12] experimentally investigated the effect of double counter twisted tape observing enhancement by double countered twisted tubes higher than single twisted tape, double co-twisted, and straight tubes for least twist ratio. Moreover, Bhuiya et al. [13] revealed that the triple twisted tape transport higher heat for small twist ratio than that of plain tubes.

Chokphoemphun et al. [14] conducted experiments for better thermal performance for counter twist instead of co-twisted arrangement and improved with increasing number of tapes. Piriyarungrod et al. [15] premeditated the effect of tapered twisted tape inserts experimentally. It was observed that, as taper angle increased, friction factor ratio and Nusselt number ratio decreased, while thermal performance factor amplified. In addition, as twist ratio decreased, Nusselt

number ratio, friction factor and thermal performance factor augmented. Tapered twisted tape with lowest taper angle and twist ratio gave highest Nusselt number ratio and friction factor ratio compared to plain tube. The thermal performance factor was found superior for lowest twist ratio and highest taper angle. Eiamsa-ard et al. [16] experimented between helical twisted tape (HTT) and conventional helical tape (CHT). It was noted that, as helical pitch ratio and twist ratio decrease, friction factor ratio and Nusselt number ratio increase, while thermal performance factor decreases. Nusselt number and friction factor was observed highest for smallest twist ratio and helical pitch ratio equated to plain tube and CHT, while thermal performance factor acquired was highest for largest twist ratio and helical pitch ratio.

Nanan et al. [17] investigated experimentally and studied regarding Co (Co-HTT) and counter (C-HTT) helical twisted tape. It was observed that, C-HTT yielded greater Nusselt Number and friction factor, whereas, Co-HTT yields higher thermal performance factor. It was concluded, that as helical pitch ratio decreased, Nusselt number and friction factor increased, whereas thermal performance factor decreased. Eiamsa-ard et al. [18] experimentally premeditated assessment between single (S-HTT), double (D-HTT) and triple (T-HTT) helical twisted tapes. Friction factor and Nusselt number amplified as width ratio increased. The thermal performance factor was highest for smallest tape width ratio 0.1 in all cases with S-HTT performing better than D-HTT and T-HTT. The heat transfer coefficient was observed highest for S-HTT than D-HTT and T-HTT.

Bhuyia et al. [19] investigated experimentally double-helical tape inserts with helix angle of 90 exhibited superior performances for particular Reynolds number. Bhuyia et al. [20] investigated the first study related to mild steel triple helical tape inserts and noted that helix angle of 90 showed better performance. Eiamsa-ard et al. [21] conducted experiment and considered the effect of helical tape insert having full length by way of and devoid of central rod and regularly spaced. For obtaining higher heat transfer rate and lower pressure drop the tape spacing ratio should be less than unity. Kumar et al. [22] studied the consequence of Circular Perforated Ring (CPR) with twisted tape insert observed that, as perforation index increased, Nusselt number decreased, friction factor decreased and thermal performance factor (TPF) increased. In addition, as pitch ratio increased, Nusselt number decreased, friction factor decreased, TPF decreased.

Abdolbaqi et al. [23] experimentally investigated for flat tube inserted with twin counter twisted tapes (CTT) and co-twisted tapes (Co-TT). Twin CTT were more effective than Co-TT with smallest twist ratio. Eiamsa-ard et al. [24] experimentally investigated peripherally cut twisted tapes (PTT) with amplification for growing depth ratio and declining width ratio. Depth ratio of cut was observed more influential and overriding over the width ratio. Eiamsa-ard et al. [25] scrutinized better performance with smallest twist ratio for peripherally cut twisted tapes (PTT). Murugesan et al. [26] observed that, horizontal wing cut twisted tape (HW-TT) performed better in relationship to vertical wing cut twisted tape (VW-TT) and plain twisted tape (PTT). Wongcharee et al. [27] performed studies for clockwise and counter-clockwise aluminum twisted tape inserts. It is observed from the study that insert with lowest twist ratio having superior thermal performance.

Ponnada et al. [28] carried out an experimental study for perforated twisted tapes with alternate axis (PATT), twisted tapes (TT), and perforated twisted tapes (PTT). It was attributed that twisted tape with alternate axis, perforation, and lowest twist ratio performs better in all aspects. Promvonge [29] experimentally studied that the enhancement efficiency obtained was higher for square cross-section than circular one. Smaller wire size had better enhancement efficiency and reduced friction factor for same pitch. It was observed that, small pitch had increased Reynolds and Nusselt number, high heat transfer rate besides high friction factor. Gunes et al. [30] experimentally noted that for equilateral triangle wire coil, highest wire side length to tube diameter ratio besides smallest pitch ratio performed better.

Keklikcioglu et al. [31] experimented on equilateral triangle wire coil placed in a manner that the vertex edged confronted the flow stream observing enhancement for highest wire length to tube diameter ratio and smallest pitch ratio. Khurana and Subudhi [32] experimented on zig-zag cut spiral tape inserts with different concentrations of Al_2O_3-water and TiO_2-water nanofluids. It was concluded that zig-zag cut spiral tape inserts significantly enhance the thermal performance without any additional penalty of friction losses. Keklikcioglu et al. [33] experimented on coiled-wire inserts located away from the tube surface observing that smallest pitch ratio and smallest wall separation distance yielded better performance. It was attributed that placing vertex of triangular cross-section wire instead of edge improves overall thermo-hydraulic performance.

Hong et al. [34] experimented for a transverse corrugated tube (TCT) with double and triple wire coils with different space ratios. Eiamsa-ard et al. [35] explored twisted tape inserts and pooled non-uniform wire coil inserts. Promvonge [36] diagnosed the effect of circular coil wire with twisted tape as turbulator. They found stating peak thermal performance factor at lowermost Reynolds number with lowermost tape twist ratio and coil pitch ratio. Ranjbhar et al. [37] experimentally investigated the heat transfer performance of city gas station heaters by utilizing twisted tape inserts. They found decrement in the destroyed exergy with twisted tapes.

Eiamsa-ard and Kiatkittipong [38] numerically investigated the thermal–hydraulic performance of TiO_2/water nanofluids for circular pipes equipped with twisted tape inserts. The reveal by using TiO_2 nanofluids led to an increase in thermal performance significantly. Yakovlev et al. [39] performed experiments for an adiabatic two-phase flow in circular pipes to investigated the enhanced heat transfer rate using twisted tape insets. They reported an intensification heat transfer rate by utilization twisted tapes with ribs. Li et al. [40] investigated thermal hydraulic parameters of a fin-tube heat exchanger with wavy shaped rib inserts. The numerical study revealed up to 40 % of enhancement by inserting wavy ribs on plain fins compared to the channel without the insert.

Dmitri et al. [41] carried out heat augmentation experimental study using straight, twisted, helical wire coil and combined tapes in tubes of fire tube boilers. Augmentation for combined type inserts was observed better than any individual insert. Further need for future work on insert geometries and pressure drop were expressed in their study.

Hakan et al. [42] carried experimental study on conical spring turbulators (CST) with three conical angles of 30°, 45° and 60° and having arrangement of converging

conical (CR), diverging conical (DR) and converging–diverging conical ring (CDR) ring, using air as working fluid for Reynold number ranging from 10 000 to 34 000. The study also mentions use of flex spring in boilers, having considerable pressure drop. The study mentions CST improves heat transfer but at the expense of pressure drop, highlighting the necessity for development of turbulator enhancing heat transfer with pressure drop consideration for application of fire tube boilers. Bilal et al. [43] experimentally studied the thermal performance and emission effects on boiler with and without smoke tubes in first pass. Also, in experimentation of first pass with smoke tubes insets were deployed, but details of insets and their thermo-hydraulic factors were not discussed. The average temperature of flue gas at exit was noted as 76.9 °C with smoke tubes using turbulators and 87.6 °C for boiler without smoke tube in first pass i.e. the difference of 11 °C was observed between the studied two models. In addition, an improvement of 1.3 % in efficiency was noted. The lowering of exit flue gas temperature led to efficiency improvement due to swirl effect of flue gases caused by inserts and additional passes. Further need for future work on inserts and efficiency improvement of boilers were expressed in their study.

The reported studies encourage the present work to explore on heat augmentation which has substantial heat transfer, lower friction factor, and higher thermal performance factor. To achieve the objective of the present study, triangular shaped helical inserts having various widths and pitches are utilized to enhance the heat transfer and reduce friction factor resulting minimum effect on accumulation of foreign particles for unclean moving fluid to reduce the fluid pumping power. Furthermore, the effect of multiple pass in addition to triangular helical strip inserts is explored to utilize the energy moving out of system which is not reported in the open literature. The results for effect of triangular shaped helical inserts and multi pass system on thermo-hydraulic performance of the system are presented in this article. The present study shows that the performance of helical inserted tube is expressively improved compared to plain tube in context of heat transfer and thermal performance. Moreover, among all the geometric parameters of the helical strip inserts under study, the Nusselt Number is more for insert having least width and tighter pitch.

2 Experimental Set-Up

The experimental set up consists of steel pipe having outer diameter of 60.3 mm, inner diameter 54.3 mm, thickness 3 mm and is divided into entrance section of 1500 mm, calming section of 1500 mm, test section of 1000 mm and exit section of 1000 mm. Air to be used as fluid for experimentation. The air enters the entrance section, flows through orifice meter installed with inclined/U-tube manometer accounting for air-flow measurement. Before entering the test section, air flows through the calm section where a fully developed flow occurs. The test section to be electrically heated for uniform heat flux through nichrome wire ($R = 1.6\Omega/m$) wound throughout the outer tube surface powered by single-phase variac transformer. The outer wall surface should be insulated to overcome the thermal losses to environment.

The wall of the tube attached with K-type thermocouples (total 8) placed 1.5 mm deep on tube thickness and axially placed at 100 mm adjacently from each other to measure the local wall temperature. The test section fitted with K-type thermocouples at start and end of test section to read the air inlet and leaving temperature of test section. The thermocouple and resistance temperature detector (RTD) set are connected to multi-channel data logger to analyze the test section parameters. A U-tube manometer tapped at inlet and exit positions of test section to read the pressure difference. The three-phase high-pressure (1HP) blower powered by inverter placed after the exit section which draws the air out of the system. The flow rate adjustment is varied by the gate valve placed before the blower. Thermo-hydraulic parameters were measured at constant heat flux and isothermal conditions while keeping the heater on and off. Moreover, it was reported in previous studies that the helical tape inserts give better heat transfer rate at higher Reynolds number under turbulent regions due to aggrandize mixing of air [20]. Therefore, the present experimental carried out for steady state conditions for Reynolds number 37 500 to 52 000. Figures 1 and 2 represent schematic diagram of experimental setup and helical strip inserts. Figures 3 and 4 represents photographic view of experimental setup and helical strip inserts.

3 Data Reduction

In the present study, the air is used as an operational fluid flowing across the insulated circular pipe under constant heat flux condition. The rate of convective heat transfer rate under steady-state condition from the internal surface of pipe is presumed to be equivalent to the heat gained by the air, assessed from the temperature change across test section and therefore, the heat balance energy equation can be described as:

$$Q_{air} = Q_{conv.} = VI \tag{1}$$

where V is voltage in volts (v) and I is current in ampere (A).

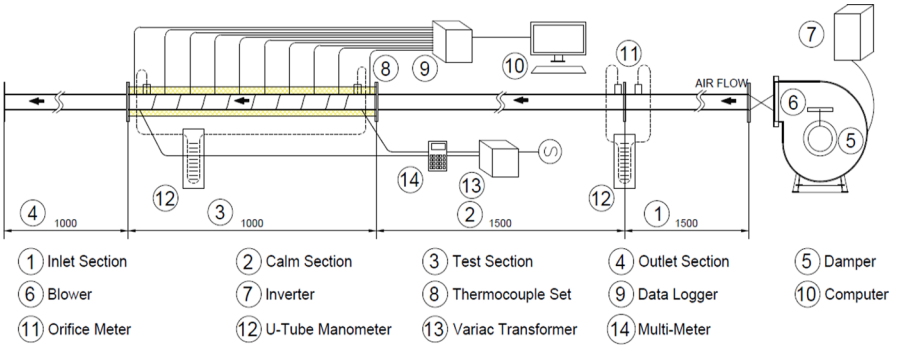

Fig. 1 Schematic diagram of experimental setup

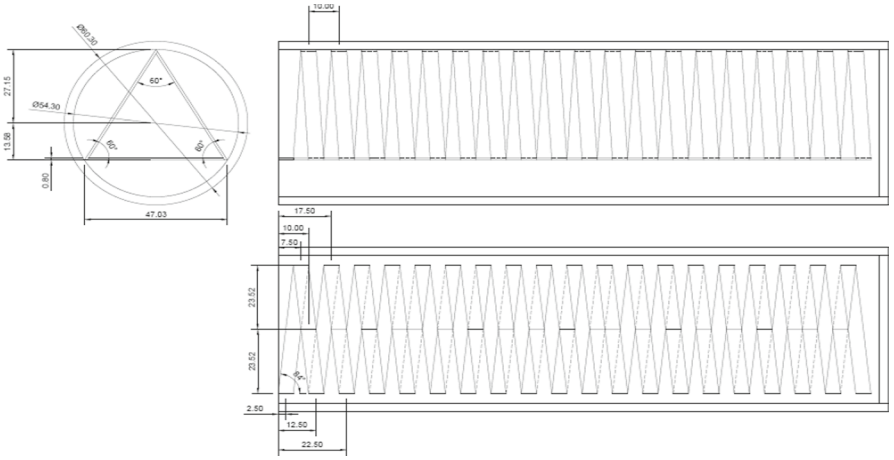

Fig. 2 Schematic diagram of helical strip inserts

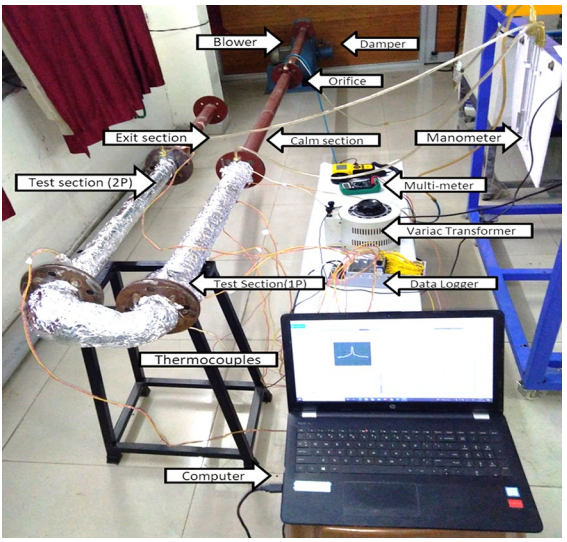

Fig. 3 Photographic view of experimental setup

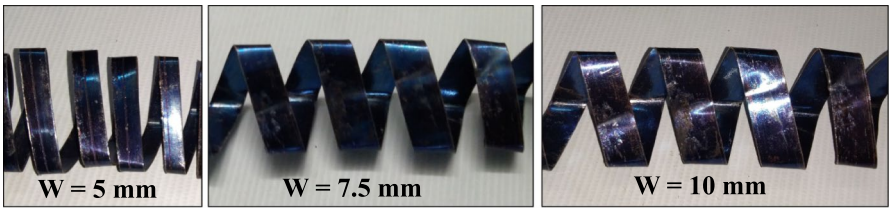

Fig. 4 Helical strip inserts with varying width

From the experimentation of test pipe under constant heat flux condition, the convective heat absorbed by air for thermal equilibrium is 1 % to 9 % lesser than the heat provided by electrical heater.

$$\left|\frac{Q_{VI-Q_{air}}}{Q_{VI}}\right| X100 \leq 1-9\% \tag{2}$$

Heat absorbed by the fluid (air) can be calculated as:

$$\mathrm{Q}_{air} = \dot{\mathrm{m}} C_{pa}(\mathrm{T_o} - \mathrm{T_i}) \tag{3}$$

where (C_p) is specific heat of air at constant pressure, $(\dot{m})$ is air mass flow rate, $(\mathrm{T_o})$ and $(\mathrm{T_i})$ are temperature at air outlet and air inlet respectively, and $(\mathrm{T_o})$ and $(\mathrm{T_i})$.

Convective heat transfer at pipe Surface can be described as:

$$Q_{conv.} = \mathrm{h\ A}_s\left(T_{wm} - T_b\right) \tag{4}$$

where $(\mathrm{T_{wm}})$ and $(\mathrm{T_b})$ are mean temperature of pipe wall and fluid respectively, (h) is convective heat transfer coefficient, and (A_s) is surface area of tube.

Bulk mean fluid temperature can be written as:

$$\mathrm{T}_b = \left(T_o + T_i\right)/2 \tag{5}$$

Mean Wall Temperature can be written as:

$$\mathrm{T}_{wm} = \sum T_{wx}/N_{tp} \tag{6}$$

where T_{wx} is the local wall temperature and T_{wm} is the average wall temperature, assessed at the exterior wall surface of test section by $N_{(tp)}$ number of thermocouples placed at 8 equally spaced locations at the exterior wall surface of the tube at the depth of 1.5 mm in tube of 3 mm thickness between the entry and exit of test tube section under uniform heat flux condition.

Average heat transfer co-efficient can be written as:

$$\mathrm{h} = \dot{\mathrm{m}}\, C_{pa}\left(\mathrm{T_o} - \mathrm{T_i}\right) / \mathrm{A}_s\left(T_{wm} - T_b\right) \tag{7}$$

Average Nusselt number can be written as:

$$\mathrm{Nu} = \mathrm{h}D_h/k \tag{8}$$

where $\left(D_h\right)$ is hydraulic diameter of the tube and (k) is the thermal conductivity of air.

Reynolds Number can be written as:

$$\mathrm{Re} = \rho u D/\mu \tag{9}$$

where (ρ) is density of fluid (air) at average temperature and (μ) is the dynamic viscosity of air.

Friction Factor can be written as:

$$\mathrm{f} = \Delta \mathrm{P} / \{(L/D)/(\rho u^2/2)\} \tag{10}$$

where (ΔP) is the measured pressure across the two ends of test section by using the difference in liquid levels in U-tube manometer.

The parameter for thermal performance of heat exchanging equipment in relationship to energy consumption affecting the operational cost of the system is evaluated by Thermal enhancement factor (TEF). The TEF is the ratio of Nusselt number of system with heat augmentation device (tube with helical insert) to that without augmentation device (plain/smooth tube), having alike pumping power. A TEF exceeding the value of 1 implicates energy savings by augmentation.

Thermal enhancement factor can be written as:

$$\eta = \left(Nu_a/Nu_0\right)/(f_a/f_0)^{\frac{1}{3}} \tag{11}$$

where (f_a) and (Nu_a) is the friction factor and Nusselt number of air obtained with helical inserts and (f_0) and (Nu_0) is the friction factor and Nusselt number of air obtained in plain tube.

4 Experimental Results and Discussion

In this section, the Nusselt number, friction factor and TEF with the variation in the Reynolds number for circular tube with triangular helical strip inserts has been discussed. The results were discussed at a constant heat flux generated through a nichrome wire of resistance 1.6Ω/m. Moreover, the results were explored for varying width of inserts, pitch of inserts, and passes (single and double).

4.1 Experimental Validation with Plain Tube Results

The presented investigation is verified by statistics acquired from thermal and pressure drop for plain tube without insert. Data of heat transfer and friction factor for specified Reynolds number obtained for plain tube from experiment is equated with the data acquired from Dittus–Boelter [44] and Gnielinski equation [45] for Nusselt number, and for friction factor Blasius and Petukhov equation [46] are considered from vulnerable literature to perform experimental validation.

Dittus–Boelter correlation:

$$\mathrm{Nu}_p = 0.023 Re^{0.8} Pr^{0.4} \tag{12}$$

Gnielinski correlation

$$\mathrm{Nu}_p = \frac{\left(\frac{f}{8}\right)(Re - 1000)Pr}{1 + 12.7\left(\frac{f}{8}\right)^{\left(\frac{1}{2}\right)}\left(Pr^{\left(\frac{2}{3}\right)} - 1\right)} \quad (3000 \leq \mathrm{Re} \leq 5 \times 10^6) \tag{13}$$

Blasius correlation:

$$f_p = 0.316Re^{-0.25} \quad (3000 \leq \mathrm{Re} \leq 20\,000) \tag{14}$$

$$f_p = 0.184Re^{-0.20} \quad (\mathrm{Re} \geq 20\,000) \tag{15}$$

Petukhov correlation:

$$f_p = (0.790 \ln Re - 1.64)^{-2} \quad (3000 \leq \mathrm{Re} \leq 5 \times 10^6) \tag{16}$$

Figure 5 and 6 depict the verification test for Nusselt number, friction factor of plain tube acquired in current work using correlations of Eqs. 12–16. From the graphs of results obtained it can be noted that, as the Reynolds number increases Nusselt number increases, while the friction factor decreases. The obtained results have similar trend to compared correlations and prior studies. For the Nusselt number of the plain tube from the present experimentation, the obtained results are in good agreement within 5 % and 11 % compared to Dittus–Boelter and Gnielinski correlations, respectively. Variation of Nusselt number between measured and Gnielinski's correlation is observed as the correlation accounts for friction losses. While the obtained friction factor for plain tubes is within 4 %, compared to both Blasius and Petukhov correlations. The obtained results are within the rationally acceptable range of below ± 14 % and ± 20 % as mentioned in previous studies [20, 21] and depict the correctness of measurement technique and presented experimental set-up.

The correlations acquired for Nusselt number (Nu_p) and friction factor (f_p) of plain tube during the presented study of triangular helical strip insert are specified in Eqs. 17 and 18, respectively.

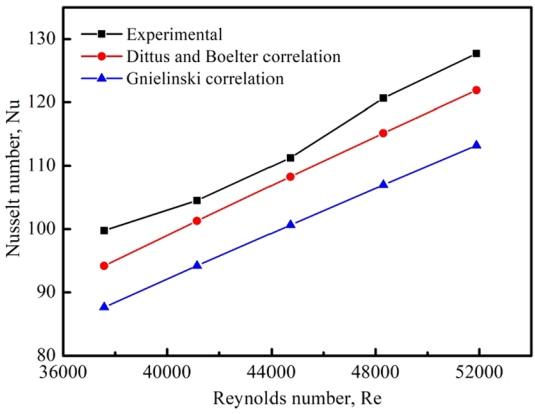

Fig. 5 Verification of Nusselt number for plain tube using the Dittus–Boelter and Gnielinski correlation

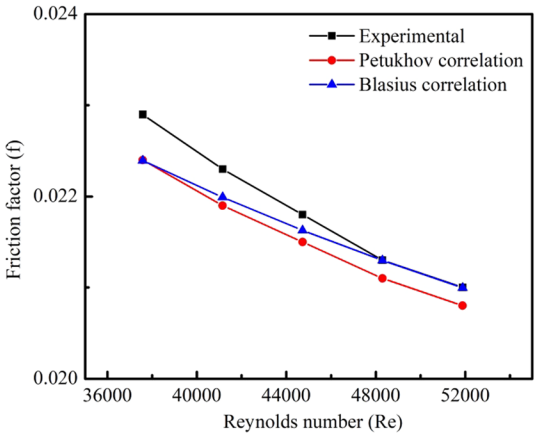

Fig. 6 Verification of friction factor data for plain tube using Petukhov and Blasius correlation

Table 1 Uncertainty of measured data and derived quantities

Measure data	Uncertainty	Derived quantity	Uncertainty
Temperature (T)	0.15 °C	Reynolds number (Re)	±2.6%
Voltage (V)	±4.8%	Heat transfer (Q)	±7.0%
Current (I)	±5.1%	Heat transfer coefficient (h)	±8.2%
Velocity (U)	±2.4%	Nusselt number (Nu)	±8.6%
Diameter	±1.1%	Friction factor (f)	±5.3%
Length of tube (L)	±1.0%		
Pressure drop (ΔP)	±1.7%		

$$\mathrm{Nu_p} = 0.02401\mathrm{Re}^{0.7995}\mathrm{Pr}^{0.3994} \tag{17}$$

$$\mathrm{f_p} = 0.4665\mathrm{Re}^{-0.2861} \tag{18}$$

4.2 Uncertainty Analysis

The uncertainty analysis of the present work is based on the method of used Moffat [47]. The formulation used for the calculation of uncertainty is represented in Eq. 19. The maximum uncertainty in the Reynolds number, Nusselt number and friction factor is given in Table 1. The obtained uncertainty of different parameters is found in acceptable range with previous studies [29, 30, 35].

$$\frac{\delta R}{R} = \sqrt{\left(a\frac{\delta X_1}{X_1}\right)^2 + \left(b\frac{\delta X_2}{X_2}\right)^2 + \left(c\frac{\delta X_3}{X_3}\right)^2 + \ldots + \left(n\frac{\delta X_n}{X_n}\right)^2} \tag{19}$$

where R is the derived quantities and X represents the measured quantities.

The uncertainties of the derived quantities can be expressed as follows:

Reynolds number uncertainty:

$$\frac{\Delta Re}{Re} = \sqrt{\left(\frac{\Delta D_h}{D_h}\right)^2 + \left(\frac{\Delta U}{U}\right)^2} \tag{20}$$

Heat transfer uncertainty:

$$\frac{\Delta Q}{Q} = \sqrt{\left(\frac{\Delta V}{V}\right)^2 + \left(\frac{\Delta I}{I}\right)^2} \tag{21}$$

Heat transfer coefficient uncertainty [48]:

$$\frac{\Delta h}{h} = \sqrt{\left(\frac{\Delta Q_{conv.}}{Q_{conv.}}\right)^2 + \left(\frac{\Delta A_S}{A_S}\right)^2 + \left(\frac{\Delta T}{T}\right)^2} \tag{22}$$

Nusselt number uncertainty:

$$\frac{\Delta Nu}{Nu} = \sqrt{\left(\frac{\Delta h}{h}\right)^2 + \left(\frac{\Delta D_i}{D_i}\right)^2 + \left(\frac{\Delta k}{k}\right)^2} \tag{23}$$

Friction factor uncertainty:

$$\frac{\Delta f}{f} = \sqrt{\left(\frac{\Delta(\Delta P)}{\Delta P}\right)^2 + \left(\frac{\Delta D_h}{D_h}\right)^2 + \left(\frac{\Delta L}{L}\right)^2 + \left(2\frac{\Delta U}{U}\right)^2} \tag{24}$$

4.3 Heat Transfer Characteristics

For the present experiment, helical strip inserts with width of 5 mm, 7.5 mm and 10 mm were considered. Each strip was experimented with two pitches (single(1P) width pitch and double (2P) width pitch) i.e., 5 mm width strip with 5 mm and 10 mm pitch, 7.5 mm width strip with 7.5 mm and 15 mm pitch, 10 mm width strip with 10 mm and 15 mm pitch. Figure 7(a) and (b) show Nusselt number (Nu) along Reynolds number (Re) for helical strip insert with single pass and double pass, respectively. It can be witnessed that the helical strip width and pitch have a noteworthy effect on Nusselt number. From Fig. 7(a) and (b) it can be noted that for all cases under consideration as Reynolds number increases there is increase in Nusselt number. It can be observed that helical strip insert shows significant augmentations for Nusselt number in association with plain tube for all cases of strip irrespective of width, pitch and number of passes.

Increasing Reynolds number increases sturdier vortex turbulent flows resulting in thinning of boundary layer, extended residence time of whirl motion, improved fluid mixing ultimately causing increased convective heat transfer. The graphs illustrate that the Nusselt number decreases for increased strip width, pitch and number of passes.

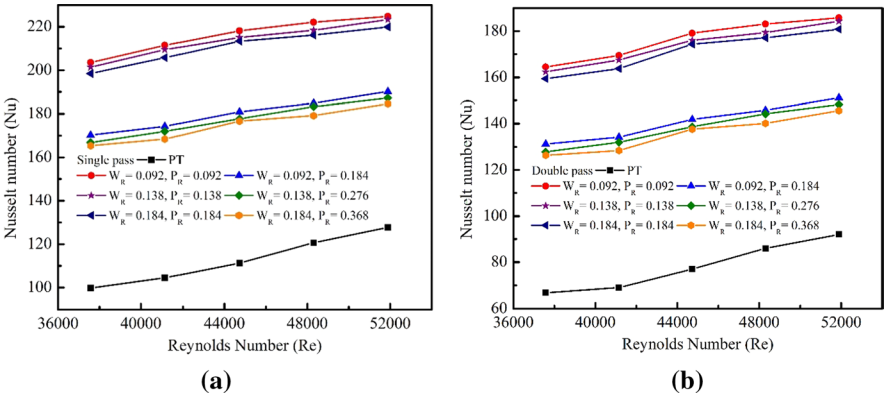

Fig. 7 Nusselt number (Nu) along Reynolds number (Re) for Helical Strip Insert (a) single pass (b) double pass

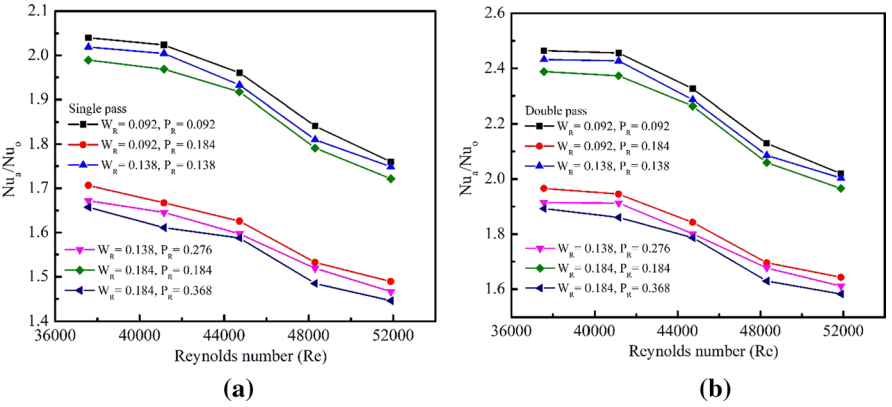

Fig. 8 Nusselt number ratio (Nu_a/Nu_o) along Reynolds number (Re) for Helical Strip Insert: (a) single pass (b) double pass

Figure 8(a) and (b) show relationship of the Nusselt number ratio (Nu_a/Nu_o) with Reynolds number (Re) for helical strip insert with single pass and double pass. It has been observed that the Nusselt number augmentation ratio (Nu_a/Nu_o) declines as the Reynolds number rises for all the experimented cases. The helical strip inserts due to their extended surface created swirl turbulent flow of the flowing fluid resulting in reducing boundary layer, increasing residence time, mixing ultimately increasing convective heat transfer compared to plain tubes. For the studied experimentation cases and Reynolds number range, of helical strip for single pass and single pitch the heat transfer over plain tubes increased by 2.04–1.76 times for ($W_R = 0.092$, $P_R = 0.092$) 2.02–1.74 times for ($W_R = 0.138$, $P_R = 0.138$) and 1.98–1.72 times for ($W_R = 0.184$, $P_R = 0.184$), respectively. Similarly, for double pitch with single pass, heat augmentation ranged from 1.71–1.49 times for ($W_R = 0.092$, $P_R = 0.184$);

1.67–1.46 times for ($W_R = 0.138$, $P_R = 0.276$) and 1.66–1.44 times for ($W_R = 0.184$, $P_R = 0.368$) respectively.

Correspondingly, the heat augmentation for double pass with single over plain tubes increased by 2.46–2.01 times for ($W_R = 0.092$, $P_R = 0.092$)2.43–1.99 times for ($W_R = 0.138$, $P_R = 0.138$) and 2.38–1.96 times for ($W_R = 0.184$, $P_R = 0.184$), respectively. Similarly for double pitch with double pass, heat augmentation ranged from 1.96–1.64 times for ($W_R = 0.092$, $P_R = 0.184$); 1.91–1.61 times for ($W_R = 0.138$, $P_R = 0.276$) and 1.89–1.56 times for ($W_R = 0.184$, $P_R = 0.368$), respectively. Nusselt number is more for single pitch than double pitch. The maximum Nusselt number was obtained for strip having 5 mm width single pitch 5 mm and single pass.

The average Nusselt number augmentation ratio (Nu_a/Nu_o) for helical strip insert with single pass and double is 1.45–2.01 and 1.58–2.46 respectively. As Reynolds number increases, the boundary layer region diminishes and reduces influence of insert. Better heat augmentation of Nusselt number enhancement ratio is more in double pass than in single pass because more heat entrapment by fluid flowing through tube due to extended residence time.

From the experimentation it has been observed that triangular helical strip insert improves convective heat transfer process as compared to plain tube, indicating the potential to reduce the heat transfer area and compactness of boiler, air preheater and other heat transfer equipment.

4.4 Fluid Flow Characteristics

Friction factor governs the performance of any heat exchanger. Figure 9(a) and (b) shows varying friction factor with Reynolds number (Re) for helical strip insert with single pass and double pass. The friction factor using helical strip inserted in tube steadily decreases with growing Reynolds number. Tube with helical strip inserts leads to higher friction factors than compared to plain tube value wash were consequence of flow obstacle and agitation, higher contact surface area with longer

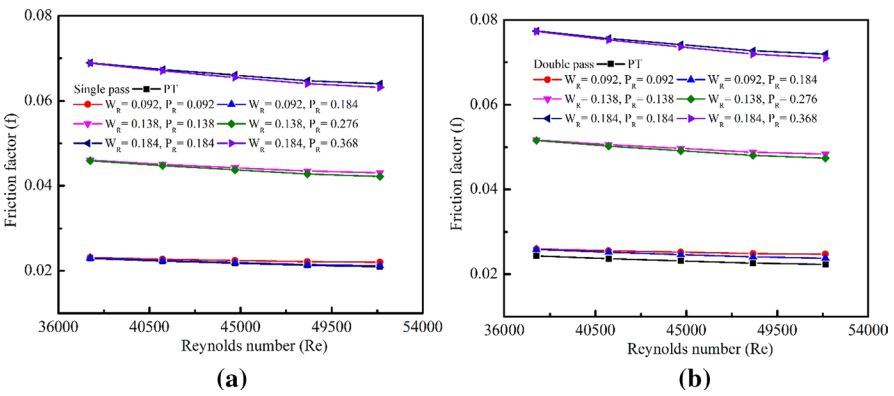

Fig. 9 Friction factor (f) with Reynolds number (Re) for helical strip Insert. (a) Single pass (b) double pass

flow path, affected by the whirling flow and indulgence of dynamic pressure of fluid owing to high viscosity loss nearby the tube wall.

Increasing pitch reduces the blockage in the frictional losses. As Reynolds number rise the friction factor was slightly high and at upper values of the Reynolds number is lowered. This may be potentially due to lower values of Reynolds flow route aiding to discharge the flow in the downstream path and thus lowers the number, conforming to lower flow rates, fluid passes through strip and formed high frictional forces due to the existing of minor vortices after inserts. For the studied experimentation cases and Reynolds number range, of helical strip for single pass and single pitch the friction factor over plain tubes increased by 1.02–1.06 times for ($W_R = 0.092$, $P_R = 0.092$); 2.01–2.05 times for ($W_R = 0.138$, $P_R = 0.138$) and 3.06–3.09 times for ($W_R = 0.184$, $P_R = 0.184$), respectively. Similarly, for double pitch with single pass, the friction factor ranged from 1.004–1.009 times for ($W_R = 0.092$, $P_R = 0.184$); 2.005–2.008 times for ($W_R = 0.138$, $P_R = 0.276$) and 3.005–3.01 times for ($W_R = 0.184$, $P_R = 0.368$) respectively.

Correspondingly, the friction factor for double pass with single over plain tubes increased by 1.0678–1.11 times for ($W_R = 0.092$, $P_R = 0.092$), 2.125–2.167 times for ($W_R = 0.138$, $P_R = 0.138$) and 3.182–3.2243 times for ($W_R = 0.184$, $P_R = 0.184$), respectively. Similarly for double pitch with double pass, friction factor ranged from 1.0624–1.0667 times for ($W_R = 0.092$, $P_R = 0.184$); 2.12–2.24 times for ($W_R = 0.138$, $P_R = 0.276$) and 3.177–3.181 times for ($W_R = 0.184$, $P_R = 0.368$), respectively. Figure 10(a) and (b) shows friction factor ratio (f_a/f_o) with Reynolds number (Re) for helical strip insert with single pass and double pass. The friction factor ratio decreases as the Reynolds number increases. The friction factor changes with the width and pitch of inserts and the higher results were obtained for inserts with the highest width and pitch, which caused a stronger whirl stream or turbulence flow and lengthy residence time in the tube. Over the range examined, the friction factors of the tube fitted with helical strip inserts were 1.1–3.2 times of the plain tube values.

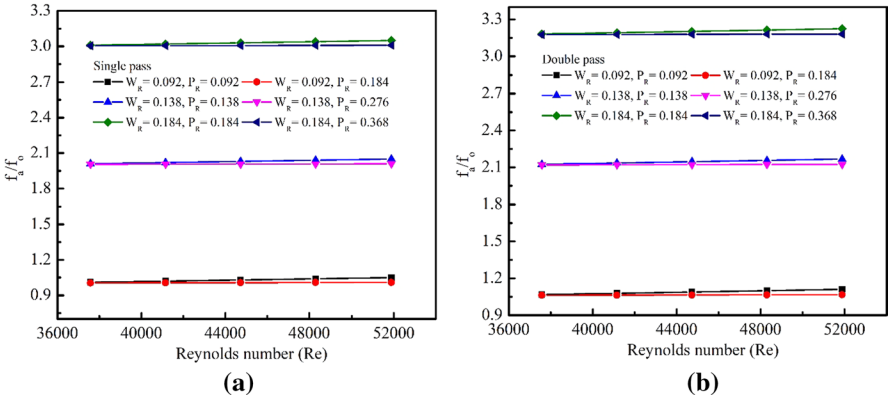

Fig. 10 Friction factor ratio (fa/fo) with Reynolds number (Re) for helical strip Insert: (a) single pass (b) double pass

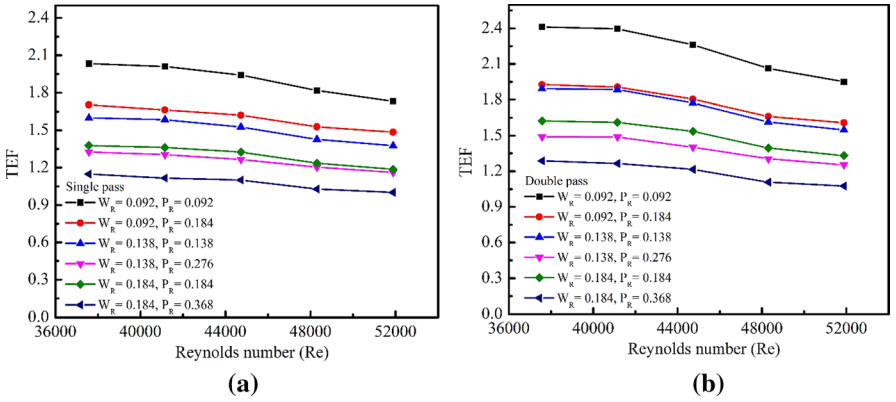

Fig. 11 Thermal enhancement factor (TEF) with Reynolds number (Re) for helical strip insert: (a) single pass (b) double pass

4.5 Thermal Enhancement Factor Evaluation

Figure 11 shows heat transfer enhancement along Reynolds number for all the cases of helical strip inserts. It is observed that TEF of helical insert strip is above unity, indicating that helical strip insert is helpful over the plain tube. TEF inclines to decrease with growing Reynolds number for all cases considered. TEF increases for lower pitch ratio, specifically at a lower Reynolds number. TEF is high for lower insert width, tight pitch and for higher number of passes. TEF for helical strip inset for single and double pass ranges from 1.01–2.01 and 1.08–2.41 respectively.

For the studied experimentation cases and Reynolds number range, of helical strip for single pass and single pitch the TEF increased by 2.03–1.732 times for ($W_R = 0.092$, $P_R = 0.092$); 1.59–1.37 times for ($W_R = 0.138$, $P_R = 0.138$) and 1.38–1.187 times for ($W_R = 0.184$, $P_R = 0.184$) respectively. Similarly, for double pitch with single pass, the friction factor ranged from 1.704–1.485 times for ($W_R = 0.092$, $P_R = 0.184$); 1.32–1.16 times for ($W_R = 0.138$, $P_R = 0.276$) and 1.148–1.013 times for ($W_R = 0.184$, $P_R = 0.368$) respectively.

Correspondingly, the TEF for double pass with single pitch over plain tubes increased by 2.41–1.95 times for ($W_R = 0.092$, $P_R = 0.092$)1.892–1.548 times for ($W_R = 0.138$, $P_R = 0.138$) and 1.624–1.331 times for ($W_R = 0.184$, $P_R = 0.184$), respectively. Similarly for double pitch with double pass, friction factor ranged from 1.93–1.61 times for ($W_R = 0.092$, $P_R = 0.184$); 1.49–1.254 times for ($W_R = 0.138$, $P_R = 0.276$) and 1.287–1.076 times for ($W_R = 0.184$, $P_R = 0.368$), respectively. Hence, higher TEF for a greater number of passes indicates energy utilization.

4.6 Development of Empirical Correlations for Prediction of Nusselt Number and Friction Factor

The correlations are presented for Nusselt number and friction factor developed from the performed experimental study of triangular helical strip insert as function

Reynolds number, Prandtl number, strip width, pitch and number of passes is formulated in Eqs. 25 and 26, respectively.

$$\mathrm{Nu}_{a(thsi)} = 3.6583 Re^{0.3732} Pr^{0.4} (W_R)^{0.2536} (P_R)^{-0.2953} \tag{25}$$

$$f_{a(thsi)} = 12.2224 Re^{0.2412} (W_R)^{1.5319} (P_R)^{-0.0136} \tag{26}$$

It is observed that the predicted empirical correlations for both the Nusselt number and friction factor are in good agreement of acceptable range within ± 15 % deviation [49] in comparison to the presented experimental data. The developed correlations (Eqs. 25 and 26) are applicable for triangular helical strip geometry of any dimension with Reynolds numbers ranging from 37 500 to 52 000. The Eqs. 25 and 26 will be helpful and useful for assessing the best-fit geometry and dimension of triangular helical strip inserts for suitable applications under consideration.

4.7 Comparison of Presented Triangular Helical Strip Work with Some of the Previous inserts Studies

The previously reported studies on inserts, encourage the present work to explore heat augmentation which has substantial heat transfer, lower friction factor, and higher thermal performance factor. Some of them are used perforated twisted tape, perforated double counter twisted tape, double counter twisted tape, triple twisted tape inserts of Bhuiya et al. [10–13], coiled square wires of Promvonge et al. [29] and Gunes et al. [30]. Figure 12 depicts the comparison of Nusselt number ratio, friction factor ratio and TEF for present triangular helical strip work with previous inserts work [10–13, 29, 30].

For perforated twisted tape [10] with a twist ratio of 1.92 and porosity of 4.5 % had better performance and heat transfer augmentation, friction factor ratio and TEF were 1.1–3.4, 1.1–3.6, and 1.25–1.59 times, respectively compared to plain tube. For perforated double counter twisted tape [11] with a twist ratio of 1.92 and porosity of 4.6 % had better performance and heat transfer augmentation, friction factor ratio, and TEF was 1.8–2.9, 1.11–3.35, and 1.08–1.44 times, respectively, compared to plain tube. For perforated double counter twisted tape [12] with a twist ratio of 1.95 had better performance and heat transfer augmentation, friction factor ratio and TEF were 1.06–2.4, 1.91–2.86, and 1.01–1.34 times, respectively, compared to plain tube. For triple twisted tape inserts [13] with a twist ratio of 1.92 had better performance and heat transfer augmentation, friction factor ratio, and TEF were 1.73–3.85, 1.91–4.2, and 1.10–1.44 times, respectively, compared to plain tube. For coiled square wires [29] with 3 mm square section and 15 mm pitch had better performance and heat transfer augmentation, friction factor ratio and TEF were 2.2–2.6, 6.2–8.0, and 1.1–1.3 times respectively compared to plain tube. For an equilateral triangle, cross-sectioned coiled wire inserts [30] with a triangle side ratio of 0.0892 and pitch ratio of 1 had better

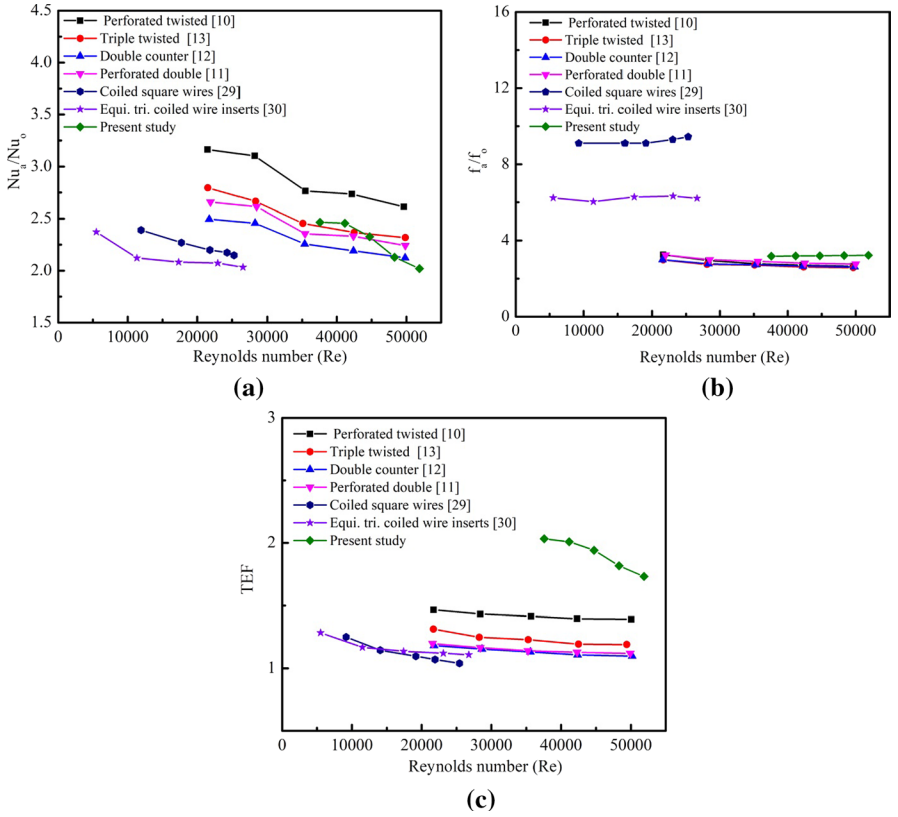

Fig. 12 Comparison of presented triangular helical strip results for single pass with previous inserts work (a) Nusselt number ratio (b) friction factor ration (c) TEF

performance and heat transfer augmentation, friction factor ratio and TEF was 1.27–2.5, 3.95–6.3 and 0.94–1.365 times, respectively, compared to plain tube.

From Fig. 12, it can be seen that though the Nusselt number ratio for the presented triangular helical strip insert is lower in comparison to the considered previous works, TEF is high because of the lower friction factor. The comparison indicates that the geometrical parameters of the insert along with dimensions influence the thermo-hydraulic performance of the insert. Therefore, from the study, it can be stated that the presented triangular helical strip insert can be considered for heat augmentation in different types of heat transfer equipment.

5 Conclusions

The presented experiment depicts heat transfer, friction factor and thermal performance factor characteristics for helical strip inserts with three widths (i.e., 5 mm, 7.5 mm and 10 mm) varied with two pitches i.e., single pitch (w = P) and double pitch

(w = 2P) with single and double pass for Reynolds number ranging from 37 500 to 52 000.

- The high intensity turbulent swirl flow creates vortex formation, disrupting formation of boundary layer, increase in residence time of fluid flow, churning and better mixing, high rate of temperature and heat transfer, increase of heating surface area which gives high convection heat transfer rate. The Nusselt number of helical strip inserts is more for inserts with lower width, tighter pitch for all geometries. Nusselt number ratio was 1.45–2.05 times for single pass and 1.55–2.45 times that of plain tube
- The friction factor is lower for insert with higher pitch. The friction factor is higher for inserts with higher width. The friction factor enhancement ratio is higher for strips with a greater number of passes, tighter pitch and more width. The increase in friction factor compared to plain tube is due to augmented surface area causing reduction in flow area, dissipation of the dynamic pressure due to flow turbulence, increase in longer flow path leading to increased residence time.
- The thermo-hydraulic performance of the helical strip insert improves for high number of passes, lower width, lower pitch. The thermal performance factor is usually high at low Reynolds number. TEF for was in the range of 1.01–2.03 and 1.08–2.41 for single pass and double pass, respectively.
- The helical strip insert configuration presented is aimed at enhancing heat transfer rate, reduce friction factor and increase thermal performance factor.

Author Contributions TA: execution of experiments and preparation of the draft of the manuscript. PZ: execution of experiments, revision of the draft. NKM: revision of the draft manuscript, rectification, editing, and supervision. AS: revision of the manuscript. All authors read and approved the final manuscript.

Funding Not applicable.

Data Availability Not applicable.

Declarations

Conflict of interest The authors declare no competing interests.

References

1. P. Zainith, N.K. Mishra, Heat Transf. Res. **52**, 16 (2021)
2. A. Painuly, N.K. Mishra, P. Zainith, J. Enhanc, Heat Transf. **29**, 1 (2022)
3. P. Zainith, N.K. Mishra, Int. J. Thermophys. **43**, 1–29 (2022)
4. P. Zainith, N.K. Mishra, Int. J. Thermophys. **42**, 1–21 (2021)
5. P. Zainith, N.K. Mishra, J. Therm. Sci. Eng. Appl. **13**, 5 (2021)
6. P. Zainith, N.K. Mishra, J. Therm. Sci. Eng. Appl. **14**, 8 (2022)

7. S. Eiamsa-Ard, C. Thianpong, P. Eiamsa-Ard, P. Promvonge, Int. Commun. Heat Mass Transf. **36**, 365–371 (2009)
8. P. Eiamsa-Ard, N. Piriyarungroj, C. Thianpong, S. Eiamsa-Ard, Case Stud Therm. Eng. **3**, 86–102 (2014)
9. J.U.J. Ahamed, M.A. Wazed, S. Ahmed, Y. Nukman, T.M.Y.S. Ya, M.A.R. Sarkar, J. Heat Transf. **133**, 4 (2011)
10. M.M.K. Bhuiya, M.S.U. Chowdhury, M. Saha, M.T. Islam, Int. Commun. Heat Mass Transf. **46**, 49–57 (2013)
11. M.M.K. Bhuiya, A.K. Azad, M.S.U. Chowdhury, M. Saha, Int. Commun. Heat Mass Transf. **74**, 18–26 (2016)
12. M.M.K. Bhuiya, A.S.M. Sayem, M. Islam, M.S.U. Chowdhury, M. Shahabuddin, Int. Commun. Heat Mass Transf. **50**, 25–33 (2014)
13. M.M.K. Bhuiya, M.S.U. Chowdhury, M. Shahabuddin, M. Saha, L.A. Memon, Int. Commun. Heat Mass Transf. **48**, 124–132 (2013)
14. S. Chokphoemphun, M. Pimsarn, C. Thianpong, P. Promvonge, Chin. J. Chem. Eng. **23**, 755–762 (2015)
15. N. Piriyarungrod, S. Eiamsard, C. Thianpong, M. Pimsarn, K.J.C.E. Nanan, Chem. Eng. Proc. **96**, 62–71 (2015)
16. S. Eiamsa-Ard, K. Yongsiri, K. Nanan, C. Thianpong, Chem. Eng. Proc. Process Intensif. **60**, 42–48 (2012)
17. K. Nanan, K. Yongsiri, K. Wongcharee, C. Thianpong, S. Eiamsa-Ard, Int. Commun. Heat Mass Transf. **46**, 67–73 (2013)
18. S. Eiamsa-Ard, K. Nanan, K. Wongcharee, K. Yongsiri, C. Thianpong, Chemi. Eng. Commun. **202**, 606–615 (2015)
19. M.M.K. Bhuiya, M.S.U. Chowdhury, J.U. Ahamed, M.J.H. Khan, M.A.R. Sarkar, M.A. Kalam, M. Shahabuddin, Int. Commun. Heat Mass Transf. **39**, 818–825 (2012)
20. M.M.K. Bhuiya, J.U. Ahamed, M.S.U. Chowdhury, M.A.R. Sarkar, B. Salam, R. Saidur, M.A. Kalam, Int. Commun. Heat Mass Transf. **39**, 94–101 (2012)
21. S. Eiamsa-ard, P. Promvonge, Sol. Energy **78**, 483–494 (2005)
22. A. Kumar, S. Singh, S. Chamoli, M. Kumar, Heat Transf. Eng. **40**, 616–626 (2019)
23. M.K. Abdolbaqi, W.H. Azmi, R. Mamat, N.M.Z.N. Mohamed, G. Najafi, Int. Commun. Heat Mass Transf. **75**, 295–302 (2016)
24. S. Eiamsa-Ard, P. Seemawute, K. Wongcharee, Exp. Therm. Fluid Sci. **34**, 711–719 (2010)
25. S. Eiamsa-ard, P. Seemawute, K. Wongcharee, Int. Heat Transf. Conf. **49378**, 547–553 (2010)
26. P. Murugesan, K. Mayilsamy, S. Suresh, Exp. Heat Transf. **25**, 30–47 (2012)
27. K. Wongcharee, S. Eiamsa-Ard, Int. Commun. Heat Mass Transf. **38**, 348–352 (2011)
28. S. Ponnada, T. Subrahmanyam, S.V. Naidu, Int. J. Therm. Sci. **136**, 530–538 (2019)
29. P. Promvonge, Energy Convers. Manage. **49**, 980–987 (2008)
30. S. Gunes, V. Ozceyhan, O. Buyukalaca, Exp. Therm. Fluid Sci. **34**, 684–691 (2010)
31. O. Keklikcioglu, V. Ozceyhan, Appl. Therm. Eng. **131**, 686–695 (2018)
32. D. Khurana, S. Subudhi, J. Therm. Sci. Eng. (2022). https://doi.org/10.1115/1.4052016
33. O. Keklikcioglu, V. Ozceyhan, Int. Commun. Heat Mass Transf. **78**, 88–94 (2016)
34. Y. Hong, J. Du, S. Wang, W.B. Ye, S.M. Huang, Int. J. Heat Mass Transf. **130**, 483–495 (2019)
35. S. Eiamsa-Ard, P. Nivesrangsan, S. Chokphoemphun, P. Promvonge, Int. Commun. Heat Mass Transf. **37**, 850–856 (2010)
36. P. Promvonge, Energy Convers. Manag. **49**, 2949–2955 (2008)
37. B. Ranjbar, M. Rahimi, F. Mohammadi, Int. J. Thermophys. **42**, 1–19 (2021)
38. S. Eiamsa-ard, K. Kiatkittipong, Int. J. Thermophys. **40**, 1–14 (2019)
39. A.B. Yakovlev, S.E. Tarasevich, A.A. Giniyatullin, A.V. Shishkin, J. Enhanc, Heat Transf. **20**, 6 (2013)
40. L. Li, X. Du, L. Yang, Y. Yang, G. Wei, J. Enhanc, Heat Transf. **23**, 6 (2016)
41. D. Neshumayev, A. Ots, J. Laid, T. Tiikma, Exp. Therm. Fluid Sci. **28**, 877–886 (2004)
42. H. Karakaya, A. Durmus, Int. J. Heat Mass Transf. **60**, 756–762 (2013)
43. B. Sungur, B. Topaloglu, Renew. Energy **143**, 121–129 (2019)
44. F.W. Dittus, L.M.K. Boelter, Int. Commun. Heat Mass Transf. **12**, 3–22 (1985)
45. V. Gnielinski, NASA STI/recon technical report A **41**, 8–16 (1975)
46. B.S. Petukhov, Adv. Heat Transf. **6**, 503–564 (1970)
47. R.J. Moffat, Exp. Therm. Fluid Sci. **1**, 3–17 (1988)

48. G.K. Poongavanam, V. Ramalingam, Int. J. Heat Mass Transf. **139**, 1–14 (2019)
49. S. Eiamsa-ard, C. Thianpong, P. Promvonge, Int. Commun. Heat Mass Transf. **33**, 1225–1233 (2006)